International Journal of Innovative Computing, Information and Control
Volume **18**, Number **4**, August **2022**

ICIC International ©2022 ISSN 1349-4198
pp. **1247–1263**

RESEARCH ON VIBRATION SUPPRESSION OF TRANSMISSION CHAIN IN WIND POWER GENERATION SYSTEM WITH GEAR CLEARANCE BASED ON INTERNAL MODEL CONTROL

Chenyang Zhou[1], Yanxia Shen[1,*] and Zaifu Wang[2]

[1]School of Internet of Things Engineering
Jiangnan University
No. 1800, Lihu Avenue, Wuxi 214122, P. R. China
7181905026@stu.jiangnan.edu.cn; *Corresponding author: shenyx@jiangnan.edu.cn

[2]School of Electrical and Electronics Engineering
Jiangsu Ocean University
No. 59, Cangwu Road, Haizhou District, Lianyungang 222005, P. R. China
jou_wangzf@jou.edu.cn

Received December 2021; revised April 2022

Abstract. *To address the vibration problem caused by gear clearance in the transmission chain of a doubly-fed wind power system, this paper uses the three-mass transmission chain with clearance to address these issues. First, we discuss the nonlinear characteristics of gear clearance and the nonlinear vibration principle. The nonlinear clearance unit is then decomposed into a linear unit and a nonlinear bounded disturbance unit. A method based on internal model control (IMC) is proposed to suppress nonlinear bounded disturbances. The nonlinear disturbance of gear clearance is suppressed by utilizing the internal model control's effective anti-disturbance capability. Vibrations caused by the transmission chain's elasticity are suppressed using an equivalent feedback controller based on the IMC controller. The simulation results demonstrate the method's effectiveness.*
Keywords: Wind power generation system, Three-mass transmission chain, Mechanical vibration suppression, Internal model control (IMC), Gear clearance

1. **Introduction.** The elasticity of the transmission chain and the gear clearance are two critical factors that contribute to transmission chain vibration. These vibrations significantly affect the transmission chain's steady-state and dynamic performance.

The servo motor drives the load via the servo system's gearbox, which in turn drives the large inertia gear via the small inertia gear. The transmission chain's elastic deformation is the primary cause of transmission chain vibration. Many studies have been conducted on the mechanism of vibration caused by transmission shaft elasticity and methods for its suppression [1-3]. The notch filter or PID control method is the most frequently used technique for suppressing mechanical vibration caused by the transmission chain's elasticity [4].

A doubly-fed wind power system's transmission chain comprises a wind turbine, a speed-raising gearbox, a generator, and a transmission shaft. The gearbox, which is a complex multi-mass transmission chain, contains three gear systems. The wind turbine drives the generator via the transmission shaft and the speed-raising gearbox through this transmission chain. In contrast to the servo system, the wind power system experiences vibration not only due to the elasticity of the transmission shaft but also due to gear clearance. However, the methods used to suppress elastic vibration cannot be used to suppress

DOI: 10.24507/ijicic.18.04.1247

the nonlinear vibration caused by gear clearance. Typically, the disturbance observer [5] is used to suppress the nonlinear vibration caused by gear clearance. The disturbance observer's principle of vibration suppression is based on the fact that a nonlinear gear clearance system N can be expressed using a combination of a linear H unit and a nonlinear bounded disturbance d unit. The specific method employs a disturbance observer to observe the nonlinear bounded disturbance d, and feedback to the input end to offset the influence of nonlinear factors in the system, thereby achieving linear performance for the N. This is a form of compensation control. The key to disturbance suppression is accurate observation and compensation. The suppression effect cannot be achieved if the disturbance is not observed correctly. As a result, a more appropriate method of disturbance suppression should be investigated.

The transmission chain structure of the wind power system is divided differently according to research emphasis. There are eight-mass [6] and six-mass [7] systems, as well as the simplest two-mass system. Consider that the wind turbine, gearbox, and generator comprise the transmission chain's three fundamental components. The three-mass transmission chain is the subject of this paper's research.

The method of suppressing the elastic vibration of transmission chain is not suitable for suppressing the nonlinear vibration of gear clearance. The method of adding disturbance observer to suppress the nonlinear vibration needs to accurately observe and compensate the disturbance signal. Aiming at the above problems, this paper uses the three-mass transmission chain of wind power systems with clearance as the research object. A method based on IMC is proposed for suppressing gear clearance nonlinear vibration. The nonlinear disturbance of gear clearance is suppressed by using the effective anti-disturbance ability of IMC, and vibration caused by the elasticity of the transmission chain is suppressed by the equivalent feedback controller based on IMC.

This paper is organized as follows. Section 2 presents a mathematical model of the wind power system's three-mass transmission chain. Section 3 analyzes the vibration principle caused by the shaft elasticity and the gear clearance of a three-mass transmission chain. Section 4 proposes methods based on IMC for suppressing gear clearance nonlinear vibration and shaft elasticity vibration. Section 5 illustrates the effectiveness of the suppressing method through simulation. At the conclusion of the paper, the conclusions are drawn.

2. Mathematical Model of the Three-Mass Transmission Chain of Wind Power System.

2.1. Transmission chain of wind power system.

The transmission chain of the wind power generation system [6,8] is shown in Figure 1.

The wind turbine is connected via a low-speed shaft to the gearbox's planetary gear train on the far left. A high-speed shaft connects the gearbox's second parallel gear train to the generator on the right. The gearbox comprises three components: a planetary gear train, a first parallel gear train, and a second parallel gear train.

To demonstrate the effect of gear clearance on the transmission chain, the gearbox's elasticity was first converted to the low-speed and high-speed shafts, respectively. An equivalent total clearance expressed the clearance effect of the three gear systems in Figure 1, so a three-mass transmission chain model with gear clearance was obtained.

Figure 2 shows a schematic diagram of the equivalent gear motion relation, in which driving gear drives driven gear through a clearance delay of $2b$ [9]. In the equivalent processing process of the three-mass drive chain model, the elasticity of the driving gear is assigned to the low-speed shaft, the elasticity of the driven gear is assigned to the high-speed shaft, the driving gear and driven gear of the gearbox become a whole, and elastic

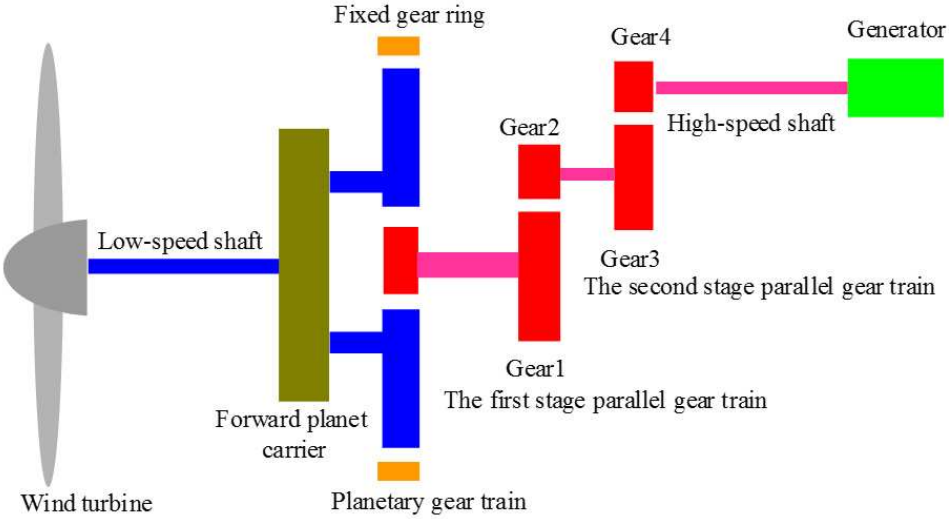

FIGURE 1. The structural diagram of the transmission chain of wind power system

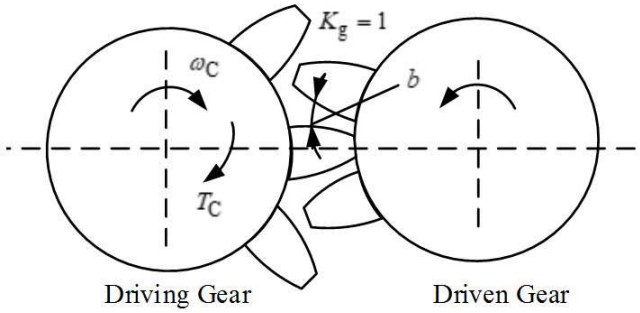

FIGURE 2. The schematic diagram of gear structure and motion relation

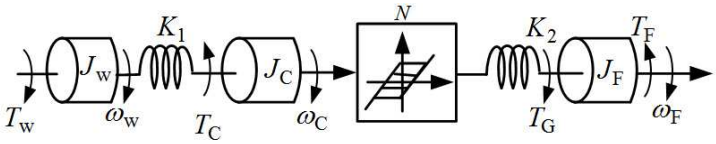

FIGURE 3. The mechanical structure schematic diagram of the three-mass transmission chain

coefficient of gear $K_g = 1$. As illustrated in Figure 3, a nonlinear clearance module N is used to represent the effect of the equivalent total clearance of three gear systems.

2.2. **Mathematical model of the three-mass transmission chain of wind power system.** The mechanical structure of the three-mass transmission chain with gear clearance is shown in Figure 3.

In Figure 3, T_W denotes the driving torque of the wind turbine, T_C represents the resistance torque of the low-speed shaft, T_G is the rotational torque of the high-speed shaft, and T_F denotes the resistance torque of the generator. ω_W represents the wind machine rotation speed, ω_C is the equivalent gear rotation speed, and ω_F denotes the generator rotation speed; J_W is the rotational inertia of the wind turbine mass block, J_C is the rotational inertia of the equivalent gear mass block, and J_F is the rotational inertia of the generator mass block. K_1 is the equivalent elastic coefficient of a low-speed shaft, and K_2 is the equivalent elastic coefficient of a high-speed shaft. The equivalent

elastic coefficient includes the converted elastic coefficient of the gearbox. The nonlinear clearance module represents the total equivalent clearance of the gearbox.

When modeling the transfer function of a wind power system's three-mass transmission chain with clearance, the gear clearance is not taken into account first. After obtaining the transmission chain's transfer function structure diagram, the nonlinear clearance unit is added. Because this paper primarily discusses transmission chain vibration, for the sake of simplicity, the gearbox transmission ratio is assumed to be one when modelling the three-mass transmission chain's transfer function.

The wind turbine, gearbox, and generator are used as research objects in Figure 3, and the following results are obtained.

1) The motion equation of the wind turbine mass block is

$$T_{\mathrm{W}} - T_{\mathrm{C}} = J_{\mathrm{W}} \frac{\mathrm{d}\omega_{\mathrm{W}}}{\mathrm{d}t} \tag{1}$$

2) The balance equation of the low-speed elastic axis is

$$T_{\mathrm{C}} = K_1 \int (\omega_{\mathrm{W}} - \omega_{\mathrm{C}})\,\mathrm{d}t \tag{2}$$

3) The motion equation of the gearbox mass block is

$$T_{\mathrm{C}} - T_{\mathrm{G}} = J_{\mathrm{C}} \frac{\mathrm{d}\omega_{\mathrm{C}}}{\mathrm{d}t} \tag{3}$$

4) The balance equation of the high-speed elastic axis is

$$T_{\mathrm{G}} = K_2 \int (\omega_{\mathrm{C}} - \omega_{\mathrm{F}})\,\mathrm{d}t \tag{4}$$

5) The motion equation of the generator mass block is

$$T_{\mathrm{G}} - T_{\mathrm{F}} = J_{\mathrm{F}} \frac{\mathrm{d}\omega_{\mathrm{F}}}{\mathrm{d}t} \tag{5}$$

The Laplace transform of Equations (1)-(5) is used to obtain Equations (6)-(10):

$$\begin{cases} J_{\mathrm{W}}\omega_{\mathrm{W}} s = T_{\mathrm{W}} - T_{\mathrm{C}} & (6) \\ T_{\mathrm{C}} = \dfrac{K_1}{s}(\omega_{\mathrm{W}} - \omega_{\mathrm{C}}) & (7) \\ J_{\mathrm{C}}\omega_{\mathrm{C}} s = T_{\mathrm{C}} - T_{\mathrm{G}} & (8) \\ T_{\mathrm{G}} = \dfrac{K_2}{s}(\omega_{\mathrm{C}} - \omega_{\mathrm{F}}) & (9) \\ J_{\mathrm{F}}\omega_{\mathrm{F}} s = T_{\mathrm{G}} - T_{\mathrm{F}} & (10) \end{cases}$$

According to Equations (6) to (10), the corresponding transfer function structure diagram can be obtained. Then, the nonlinear clearance module is added to the structure diagram. The transfer function structure diagram of the three-mass transmission chain of the wind power system with gear clearance is obtained, as shown in Figure 4.

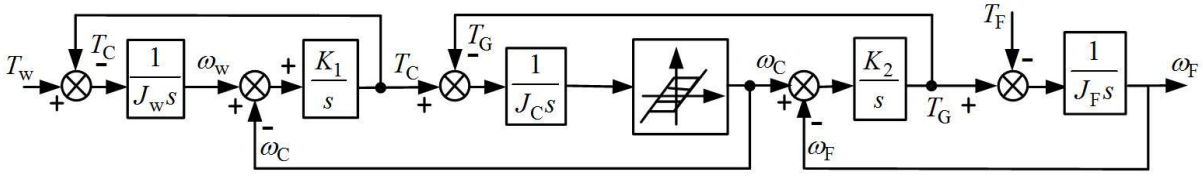

FIGURE 4. The transfer function structure diagram of the three-mass transmission chain of the wind power system with a clearance

3. **Vibration Analysis of Transmission Chain in Wind Power System.** In the transmission chain, the elasticity and gear clearance will cause the vibration of the transmission chain.

3.1. **Elastic vibration analysis of three-mass transmission chain of wind power system.** According to Equations (6)-(10), Equation (11) between the speed of the generator and the torque of the wind turbine can be obtained, from which its vibration can be analyzed.

While analyzing the relationship of $\omega_{\mathrm{F}}/T_{\mathrm{W}}$, let $T_{\mathrm{F}}=0$, we can get

$$\frac{\omega_{\mathrm{F}}}{T_{\mathrm{W}}}=\frac{K_1K_2}{J_{\mathrm{W}}J_{\mathrm{C}}J_{\mathrm{F}}s^5+(J_{\mathrm{W}}J_{\mathrm{F}}K_1+J_{\mathrm{C}}J_{\mathrm{F}}K_1+J_{\mathrm{W}}J_{\mathrm{C}}K_2+J_{\mathrm{W}}J_{\mathrm{F}}K_2)s^3+(J_{\mathrm{W}}K_1K_2+J_{\mathrm{C}}K_1K_2+J_{\mathrm{F}}K_1K_2)s} \tag{11}$$

As shown from the structure in Figure 4, the three-mass transmission chain is formed by two two-mass systems with the same structure in series. It can be decomposed into two two-mass systems in series by transforming Equation (11). The transfer function between wind turbine driving torque T_{W} and generator speed ω_{F} can also be expressed by Equation (12).

$$\frac{\omega_{\mathrm{F}}}{T_{\mathrm{W}}}=\frac{1}{J_{\mathrm{W}}s}\cdot\frac{K_1K_2}{s^4+(\omega_{\mathrm{r1}}^2+\omega_{\mathrm{r2}}^2)s^2+\omega_{\mathrm{r1}}^2\omega_{\mathrm{r2}}^2}=\frac{1}{J_{\mathrm{W}}s}\cdot\frac{K_1\cdot K_2}{(s^2+\omega_{\mathrm{r1}}^2)(s^2+\omega_{\mathrm{r2}}^2)} \tag{12}$$

In this Equation (12), ω_{r1} and ω_{r2} are the resonant frequencies of the first and second two-mass systems.

Similarly, the relationship between wind turbine speed and driving torque $\omega_{\mathrm{W}}/T_{\mathrm{W}}$ is shown in Equation (13).

$$\frac{\omega_{\mathrm{W}}}{T_{\mathrm{W}}}=\frac{J_{\mathrm{C}}J_{\mathrm{F}}s^4+(J_{\mathrm{F}}K_1+J_{\mathrm{C}}K_2+J_{\mathrm{F}}K_2)s^2+K_1K_2}{J_{\mathrm{W}}J_{\mathrm{C}}J_{\mathrm{F}}s^5+(J_{\mathrm{W}}J_{\mathrm{F}}K_1+J_{\mathrm{C}}J_{\mathrm{F}}K_1+J_{\mathrm{W}}J_{\mathrm{C}}K_2+J_{\mathrm{W}}J_{\mathrm{F}}K_2)s^3+(J_{\mathrm{W}}K_1K_2+J_{\mathrm{C}}K_1K_2+J_{\mathrm{F}}K_1K_2)s} \tag{13}$$

Equation (13) also has two resonance points because it has the same denominator as Equation (11).

A two-mass transmission chain should have a single resonance point, while a three-mass transmission chain should have two. When a resonant point exists, it indicates that there is vibration.

3.2. **The vibration caused by gear clearance of transmission chain in wind power system.** Gear clearance in a wind power system's transmission chain is a nonlinear characteristic. The nonlinear characteristics of the gear clearance [10] and their effect [11] on the control system are illustrated in Figure 5. The input and output relationships for gear clearance are shown in Figure 5(a), as shown in Equation (14).

$$q=\begin{cases}k(v-b); & \dfrac{\mathrm{d}q}{\mathrm{d}t}>0\\ k(v+b); & \dfrac{\mathrm{d}q}{\mathrm{d}t}<0\\ q_{\mathrm{m}}\mathrm{sgn}(v); & \dfrac{\mathrm{d}q}{\mathrm{d}t}=0\end{cases} \tag{14}$$

In the characteristics shown in Figure 5(a), the input is the position v of the driving gear, the output is the position q of the driven gear, $2b$ is the total clearance in the transmission chain, and the characteristic slope is k.

There are two main influences of gear clearance on control system.

1) Decrease in output signal amplitude and introduce phase lag. As illustrated in Figure 5(b), the output signal is limited by the influence of q_{m} on gear clearance characteristics. Due to the influence of the gear clearance $2b$, the output signal lags behind the input signal in phase by an angle of φ. Thus, the stability and dynamic performance of the system are affected, and the system's instability is increased.

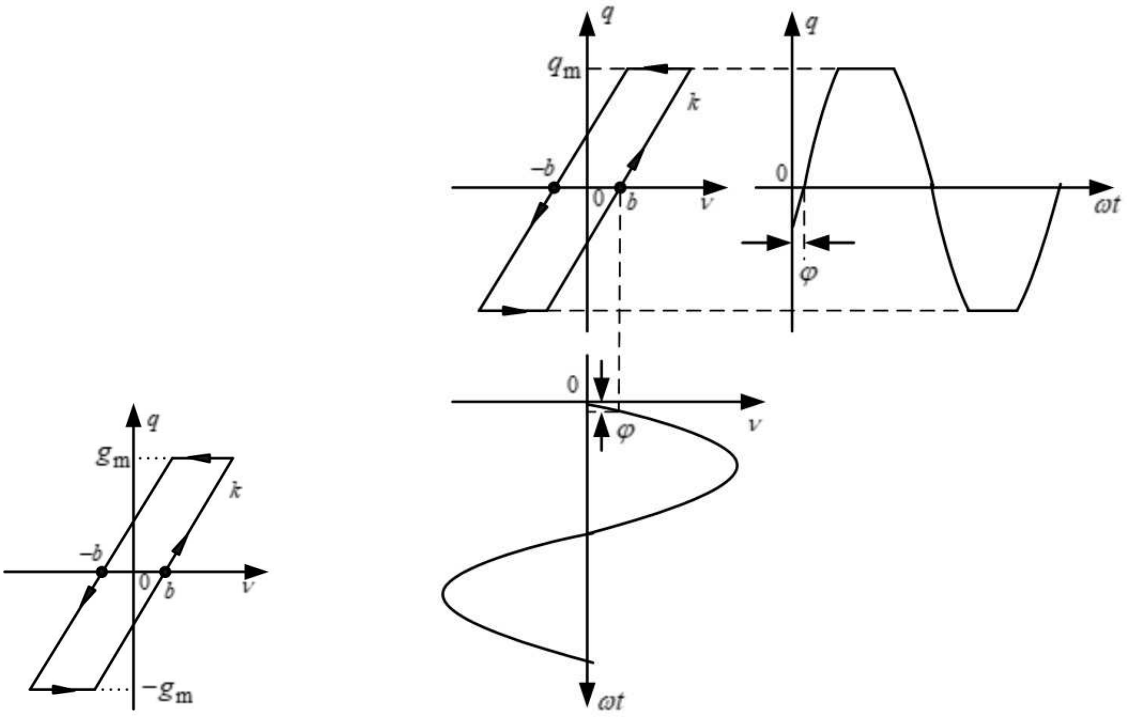

(a) Gear clearance nonlinear characteristics

(b) Influence of gear clearance on the output signal

FIGURE 5. The nonlinear characteristics and influence on output signals with gear clearance

2) When there is nonlinearity in the gear clearance, the three-mass transmission chain transitions from a linear to a nonlinear state, as illustrated in Figure 4, and vibration may occur.

3.3. **Experimental verification of vibration of three-mass transmission chain in wind power system.**

3.3.1. *Elastic vibration experiment of the three-mass transmission chain.* Figure 6 illustrates the Bode diagram of the generator side of the three-mass transmission chain using Equation (11). Table 1 contains the parameters [7] for drawing the Bode diagram.

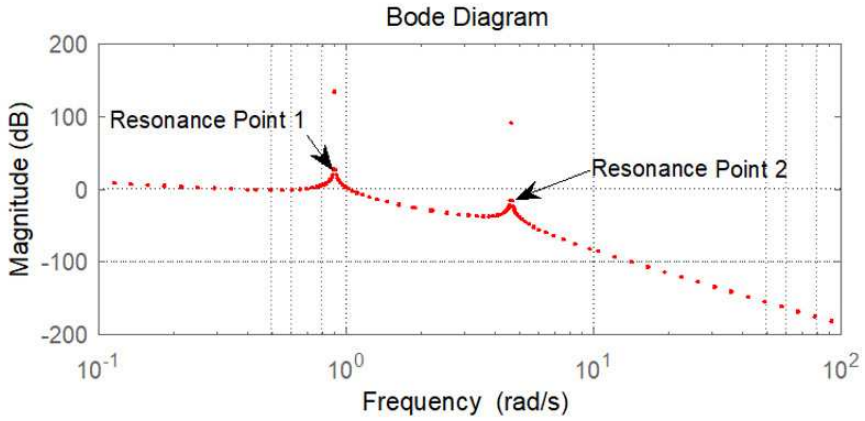

FIGURE 6. The Bode diagram of the three-mass transmission chain of the generator side

TABLE 1. The simulation experiment parameters

No.	Parameter	Value
1	J_W (kg·m^2)	2.6
2	J_C (kg·m^2)	0.272
3	J_F (kg·m^2)	0.505
4	K_1 (N·m/rad)	0.516
5	K_2 (N·m/rad)	3.51
6	$2b$ (rad)	0.2

According to the results in Figure 6, the three-mass transmission chain contains two resonance points, which is consistent with the theoretical analysis. Due to the presence of resonance points, the system's response at the characteristic frequency becomes more intense. When there are resonant points, vibration occurs.

3.3.2. *Experimental verification of nonlinear vibration of gear clearance.* To verify the effect of gear clearance nonlinearity on transmission chain performance, the output of the three-mass transmission chain transfer function in Figure 4 was subtracted from the system output for the same parameters without clearance, thereby creating an experimental system capable of verifying nonlinear clearance vibration. Figure 7 illustrates the simulation experiment scheme, and Figure 8 illustrates the generator speed deviation vibration waveform caused by gear clearance nonlinearity.

As illustrated in Figure 8, the clearance causes the system's output to vibrate.

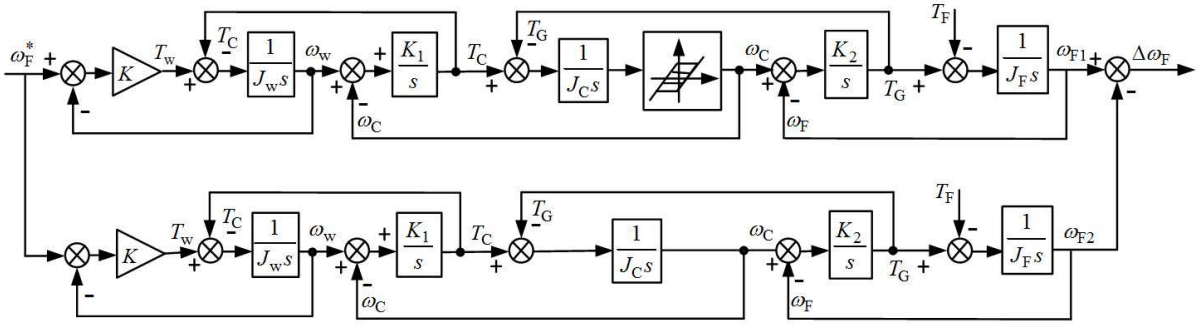

FIGURE 7. Experimental scheme of nonlinear vibration of gear clearance

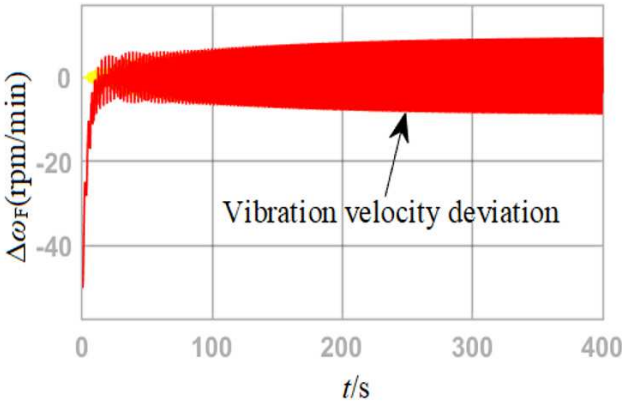

FIGURE 8. Generator speed deviation vibration waveform caused by nonlinearity of gear clearance

4. **Methods to Suppress Vibration of Transmission Chain in Wind Power System.** The speed controller method is typically used to eliminate vibration in a wind power system caused by the elasticity of the transmission chain. The speed controller can adjust the pitch angle of the wind turbine blades to adjust the driving torque applied to the blades and thus control the wind turbine driving torque T_{W}. This paper will implement the speed controller using an equivalent feedback controller based on IMC.

4.1. **Equivalence of gear clearance nonlinearity.** In Figure 5, the role of nonlinear gear clearance N in the system can be represented by the equivalent unit in the dotted box in Figure 9, where N is decomposed into two parts, $N = H + d$ [5,10].

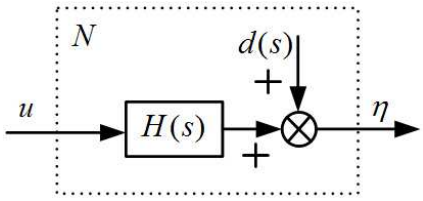

FIGURE 9. The nonlinear model of gear clearance

$H(s)$ is a linear time-invariant unit, whereas $d(s)$ is a nonlinear time-varying unit, representing a bounded disturbance. When the nonlinearity of the gear clearance is expressed as the bounded disturbance $d(s)$, the control theory method can be used to eliminate the influence of the nonlinear disturbance of the gear clearance so that N presents a linear performance.

The clearance characteristics N of the transmission chain in the wind power system are shown in Figure 10.

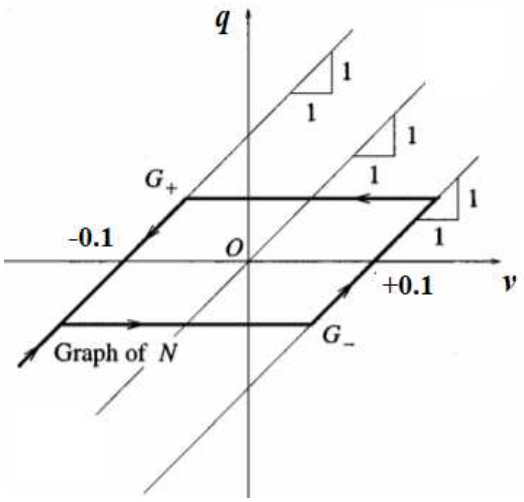

FIGURE 10. Equivalence of clearance characteristics

Obviously, the graph of N lies between or on two parallel lines $G_+(v) = kv + b$ and $G_-(v) = kv - b$ for all v. Thus, N can be decomposed into $N = H + d$, where the transfer function of the linear part is $H(s) = k$, that is, the straight line passing through the origin of coordinates in the figure. $d(s)$ is a nonlinear disturbance function bounded by b, which in this case is $2b = 0.2$. For the convenience of transformation, the slope k of the clearance characteristic is set to 1. Then, the nonlinear unit N can be represented by $H(s) = 1$ and

the nonlinear bounded disturbance function $d(s)$ in the dotted box in Figure 12(b). That is, the nonlinear factor of gear clearance can be seen as the disturbance of the system.

It is demonstrated that the nonlinear clearance factor can be equivalent to bounded disturbance. As a result, a control strategy with a disturbance suppression function is proposed to eliminate vibration caused by transmission chain gear clearance. IMC is a type of control strategy that is capable of effectively rejecting disturbances. Additionally, it can be used as a speed controller to suppress vibration caused by the transmission chain's elasticity.

4.2. **Principle of IMC to suppress nonlinear disturbance of gear clearance.** IMC is a control strategy that has a good performance of suppressing unmeasured disturbance [12]. It is particularly well suited for the suppression of nonlinear disturbances in gear clearance.

The structure of a common feedback control system is shown in Figure 11. $C(s)$ is the feedback controller, $G(s)$ is the controlled object, $d(s)$ is the unmeasured disturbance, $R(s)$ and $Y(s)$ are the input and output signals of the control system, respectively. As illustrated in Figure 11, because the feedback signal is directly derived from the system's output, the influence of $d(s)$ on the output cannot be distinguished from that of other factors in the feedback, and the disturbance cannot be effectively controlled.

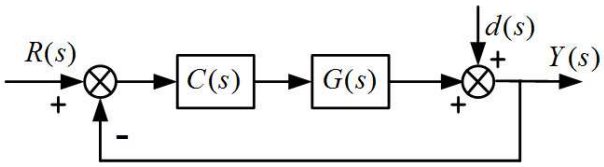

FIGURE 11. Structural diagram of common feedback control system

When Figure 11 is transformed equivalently, the IMC structure shown in Figure 12 is obtained, where $\hat{G}(s)$ is the prediction model of the controlled object, and $C_{\mathrm{IMC}}(s)$ is the IMC controller.

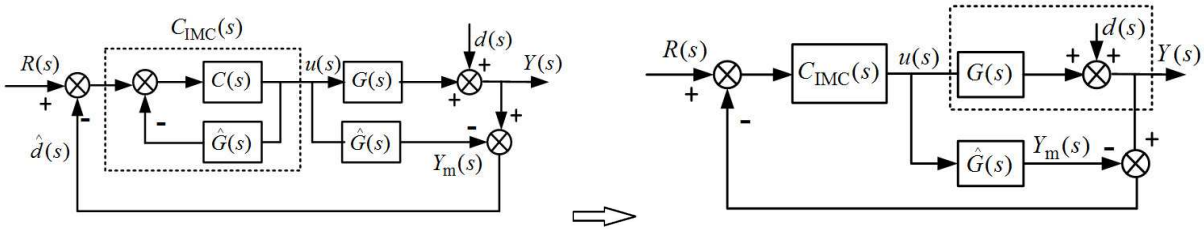

FIGURE 12. The structure diagram of IMC

The dotted box in Figure 12(a) is the IMC controller and the transfer function

$$C_{\mathrm{IMC}}(s) = \frac{C(s)}{1 + \hat{G}(s)C(s)} \tag{15}$$

From Figure 12(b), the inhibition effect of IMC on disturbance can be analyzed [13,15].

1) IMC can adjust the output deviation caused by unmeasured disturbance $d(s)$.

When the disturbance $d(s)$ occurs, the system is equipped with a feedback adjustment mechanism that suppresses the unmeasured disturbance $d(s)$. For example,

$$d(s) \uparrow\rightarrow Y(s) \uparrow\rightarrow \hat{d}(s)[= Y(s) - Y_{\mathrm{m}}(s)] \uparrow\rightarrow \left[R(s) - \hat{d}(s)\right] \downarrow\rightarrow u(s) \downarrow\rightarrow Y(s) \downarrow$$

2) When the model is matched with the controlled object, that is $\hat{G}(s) = G(s)$, and $C_{\mathrm{IMC}}(s) = \hat{G}^{-1}(s)$, the system can overcome any unmeasured disturbance $d(s)$ and achieve no deviation tracking for any input $R(s)$. For example, as illustrated in Figure 12(b),

$$Y(s) = \frac{C_{\mathrm{IMC}}(s)G(s)}{1 + C_{\mathrm{IMC}}(s)\left[G(s) - \hat{G}(s)\right]}R(s) + \frac{1 - C_{\mathrm{IMC}}(s)\hat{G}(s)}{1 + C_{\mathrm{IMC}}(s)\left[G(s) - \hat{G}(s)\right]}d(s) \tag{16}$$

If the model is matched with the controlled object and $C_{\mathrm{IMC}}(s) = \hat{G}^{-1}(s)$ can be realized, Equation (16) becomes $Y(s) = R(s)$, and the output of the system is always equal to the input; it is independent of the disturbance $d(s)$.

4.3. **Design of IMC controller and feedback controller [12,14,15].**

1) IMC controller design.

The following are the steps involved in the design of an IMC controller: First, a stable ideal controller is designed without regard for the system's robustness or constraints; Second, a low pass filter $L(s)$ is added to stabilize the system and to achieve the desired dynamic performance. The structure and parameters of $L(s)$ are adjusted to achieve the desired dynamic performance.

When the prediction model $\hat{G}(s)$ of the controlled object is known, the IMC controller can be calculated by the following formula:

$$C_{\mathrm{IMC}}(s) = \frac{C(s)}{1 + \hat{G}(s)C(s)} = \hat{G}^{-1}(s)L(s) \tag{17}$$

where $L(s)$ is a low-pass filter.

2) Feedback controller design.

The equivalent transformation of the IMC structure diagram in Figure 12(b) into the feedback control structure diagram in Figure 13 can obtain the equivalent feedback controller $C(s)$. The transfer function of the feedback controller is as follows:

$$C(s) = \frac{C_{\mathrm{IMC}}(s)}{1 - \hat{G}(s)C_{\mathrm{IMC}}(s)} \tag{18}$$

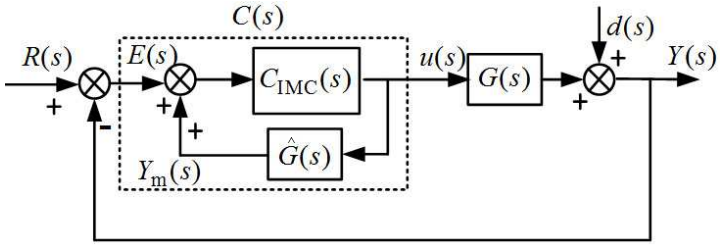

FIGURE 13. Equivalent structure diagram of feedback control

4.4. **Design of IMC controller and feedback controller for generator side.** To design the generator side IMC controller and feedback controller, the controlled object $G_2(s) = \omega_{\mathrm{F}}/T_{\mathrm{W}}$ (ratio of the generator speed to wind turbine torque) and the clearance nonlinear disturbance $d(s)$ must be transformed into the form shown in the dot-crossed box in Figure 12(b).

4.4.1. *Structural diagram transformation of three-mass transmission chain for generator side.* $T_F = 0$ was substituted into Figure 4, and the clearance nonlinearity in Figure 4 was replaced by the equivalent unit in Figure 9, resulting in Figure 14(a). $H(s) = 1$ was substituted into Figure 14(a), and after a series of equivalent transformations, Figure 14(b) was finally obtained.

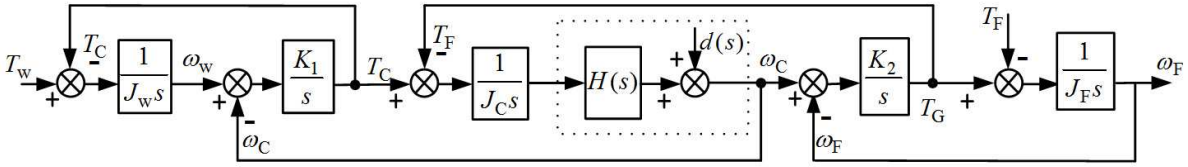

(a) Equivalent transformation of structure diagram (1)

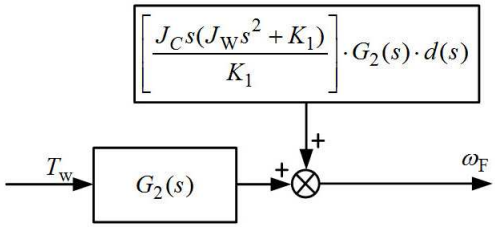

(b) Equivalent transformation of structure diagram (2)

FIGURE 14. Equivalent transformation of structure diagram of the three-mass transmission chain of wind power system

In Figure 14(b),

$$G_2(s) = \frac{\omega_F}{T_W} = \frac{K_1 K_2}{J_W J_C J_F s^5 + (J_W J_F K_1 + J_C J_F K_1 + J_W J_C K_2 + J_W J_F K_2)\, s^3 + (J_W K_1 K_2 + J_C K_1 K_2 + J_F K_1 K_2)\, s}$$

4.4.2. *Design of IMC controller and feedback controller for generator side.* As can be seen from the expression of $G_2(s)$, $G_2(s)$ is a minimum phase system without zeros in the right half-plane. Then the controlled object $G_2(s)$ can be decomposed into $G_2(s) = G_{2+}(s) \cdot G_{2-}(s)$, where $G_{2+}(s) = 1$. Substituting the parameters in Table 1, then we have

$$G_{2-}(s) = G_2(s) = \frac{1.863}{0.357s^5 + 8.04s^3 + 6.29s}$$

To make the order of the numerator and denominator of the transfer function of the controlled object close, the low-pass filter can be selected as follows:

$$L(s) = \frac{1}{(\lambda s + 1)^5} \tag{19}$$

1) Design of IMC controller $C_{\text{IMC-F}}(s)$.

The designed IMC controller $C_{\text{IMC-F}}(s)$ is

$$\begin{aligned} C_{\text{IMC-F}}(s) &= \hat{G}_2^{-1}(s) L(s) \\ &= \frac{0.357s^5 + 8.04s^3 + 6.29s}{1.863(\lambda s + 1)^5} \\ &= \frac{0.1916s^5 + 4.32s^3 + 3.376s}{(\lambda s + 1)^5} \end{aligned} \tag{20}$$

2) Design of feedback controller $C_F(s)$.

The designed feedback controller $C_{\mathrm{F}}(s)$ is

$$\begin{aligned} C_{\mathrm{F}}(s) &= \hat{G}_2^{-1}(s)\frac{1}{L^{-1}(s)-1} \\ &= \frac{0.357s^5+8.04s^3+6.29s}{1.863\left[(\lambda s+1)^5-1\right]} \\ &= \frac{0.1914s^4+4.32s^2+3.376}{\lambda^5 s^4+5\lambda^4 s^3+10\lambda^3 s^2+10\lambda^2 s+5\lambda} \end{aligned} \tag{21}$$

By substituting $\lambda = 0.01$, the generator side IMC controller $C_{\text{IMC-F}}(s)$ and feedback controller $C_{\mathrm{F}}(s)$ can be obtained.

4.5. **Design of IMC controller and feedback controller for wind turbine side.** Similarly, the controlled object $G_1(s)$ for the wind turbine side can be obtained by substituting parameters in Table 1.

$$G_{1-}(s) = G_1(s) = \frac{0.1374s^4+3.07s^2+1.863}{0.357s^5+8.04s^3+6.29s}$$

The low-pass filter is selected as $L(s) = \frac{1}{\lambda s+1}$, so that the order of the numerator and denominator of the transfer function of the controlled object is close.

1) Design of IMC controller $C_{\text{IMC-W}}(s)$.

The designed IMC controller $C_{\text{IMC-W}}(s)$ is

$$C_{\text{IMC-W}}(s) = \hat{G}_{1-}^{-1}(s)L(s) = G_{1-}^{-1}(s)L(s) = \frac{0.357s^4+8.04s^2+6.29}{0.1374s^4+3.07s^2+1.863}\cdot\frac{s}{\lambda s+1} \tag{22}$$

2) Design of feedback controller $C_{\mathrm{W}}(s)$.

The designed feedback controller $C_{\mathrm{W}}(s)$ is

$$C_{\mathrm{W}}(s) = \hat{G}_1^{-1}(s)\frac{1}{L^{-1}(s)-1} = \frac{0.357s^4+8.04s^2+6.29}{0.1374s^4+3.07s^2+1.863}\cdot\frac{1}{\lambda} \tag{23}$$

By substituting $\lambda = 0.01$, the wind turbine side IMC controller $C_{\text{IMC-W}}(s)$ and feedback controller $C_{\mathrm{W}}(s)$ can be obtained.

5. Simulation Experiment and Result Analysis.

5.1. Speed experiment of wind turbine and generator with gear clearance.

1) Schema experimental. According to Figure 4, a nonlinear gear clearance unit is connected behind the gear, and the wind turbine speed is controlled via negative feedback. The experimental design is depicted in Figure 15(a). The transmission chain parameters are listed in Table 1. The PID parameters for the speed controller are taken from [16] and are not designed using the IMC method.

2) Experimental results and analysis. Figure 15(b) shows the speed waveform of the wind turbine. In Figure 15(b), ω_{W} is the wind turbine speed waveform, and $\omega_{\text{W-ref}}$ is the reference speed waveform of the wind turbine. Figure 15(c) shows the generator speed waveform. In Figure 15(c), ω_{F} is the actual speed waveform of the generator. Since the gear clearance is located behind the wind turbine, there is some wind turbine speed vibration, but the vibration amplitude is minimal, as illustrated in Figure 15(b). The generator speed behind the gear clearance vibrates greatly, as shown in Figure 15(c). Conventional PID speed controllers do not eliminate these vibrations.

5.2. Generator side IMC and feedback control experiments.

1) Schema experimental. The Simulink simulation schema for the experiment was set up according to Figures 12(b) and 13.

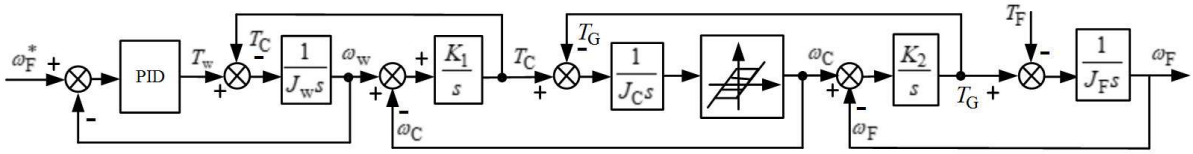

(a) The wind turbine speed feedback control system

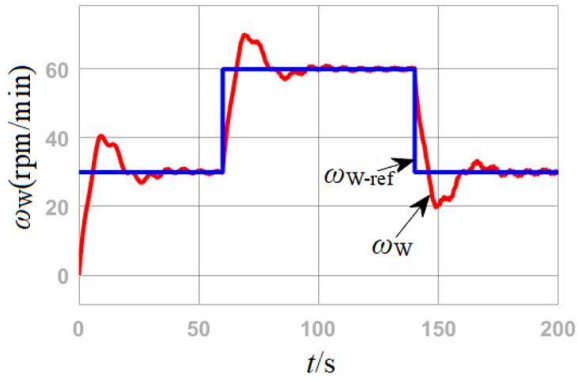

(b) Wind turbine speed waveform

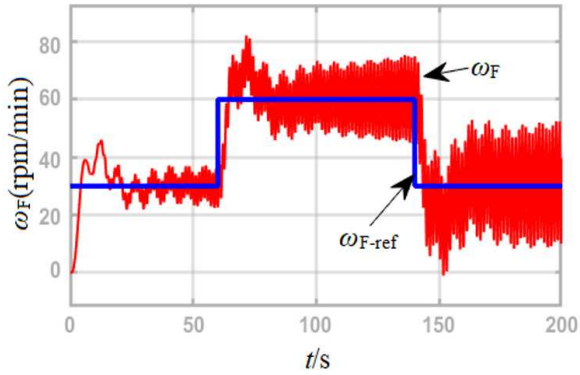

(c) Generator speed waveform

FIGURE 15. The wind turbine speed feedback control system and speed waveform of three-mass transmission chain with clearance

As shown in Figure 14(b), the controlled object's transfer function is as follows:

$$G_2(s) = \frac{1.863}{0.357s^5 + 8.04s^3 + 6.29s}$$

According to Equation (20), get that IMC controller $C_{\text{IMC-F}}(s)$ is

$$C_{\text{IMC-F}}(s) = \frac{0.1916s^5 + 4.32s^3 + 3.376s}{(\lambda s + 1)^5}, \text{ where } \lambda = 0.01$$

According to Equation (21), get that feedback controller $C_F(s)$

$$C_F(s) = \frac{0.1914s^4 + 4.32s^2 + 3.376}{\lambda^5 s^4 + 5\lambda^4 s^3 + 10\lambda^3 s^2 + 10\lambda^2 s + 5\lambda}, \text{ where } \lambda = 0.01$$

2) Experimental results and analysis. The generator speed waveform was obtained as illustrated in Figures 16(a) and 16(b).

As illustrated in Figure 16(a), when $\lambda = 0.01$, the speed waveform of the generator which is controlled by IMC basically coincides with the input speed, and the output has a good following performance to the input. As shown in Figures 16(a) and 16(b), waveforms of equivalent feedback control and IMC are consistent.

Additionally, step, sine wave, and random function disturbance signals are used to conduct the system's disturbance rejection experiment. It is discovered that disturbance signals have little effect on the output, indicating that the IMC performs well in terms of disturbance rejection.

5.3. **Wind turbine side IMC and feedback control experiments.**

1) Schema experimental. According to Figures 12(b) and 13, the Simulink simulation model for the experiment was set up.

Similar to Figure 14(b), the transfer function of the controlled object is as follows:

$$G_1(s) = \frac{0.1374s^4 + 3.07s^2 + 1.863}{0.357s^5 + 8.04s^3 + 6.29s}$$

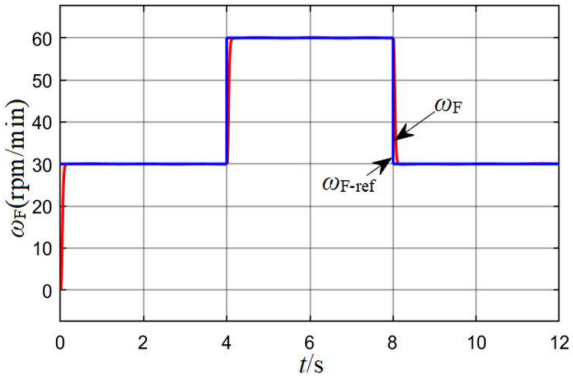

(a) The generator speed waveform based on IMC

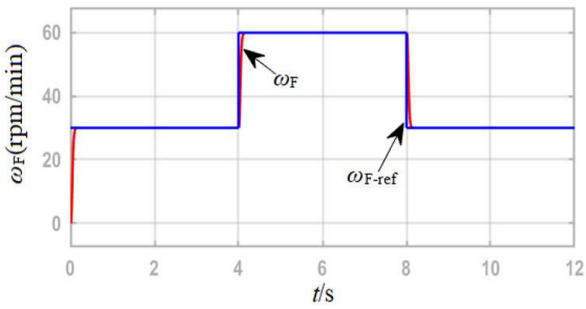

(b) The generator speed waveform based on feedback control

FIGURE 16. The speed waveform of generator based on IMC and equivalent feedback control

According to Equation (22), the IMC controller $C_{\text{IMC-W}}(s)$ is

$$C_{\text{IMC-W}}(s) = \frac{0.357s^4 + 8.04s^2 + 6.29}{0.1374s^4 + 3.07s^2 + 1.863} \cdot \frac{s}{\lambda s + 1}, \text{ where } \lambda = 0.01$$

According to Equation (23), the feedback controller $C_{\text{W}}(s)$:

$$C_{\text{W}}(s) = \frac{0.357s^4 + 8.04s^2 + 6.29}{0.1374s^4 + 3.07s^2 + 1.863} \cdot \frac{1}{\lambda}, \text{ where } \lambda = 0.08$$

2) Experimental results and analysis. The wind turbine speed waveform was obtained as shown in Figures 17(a) and 17(b).

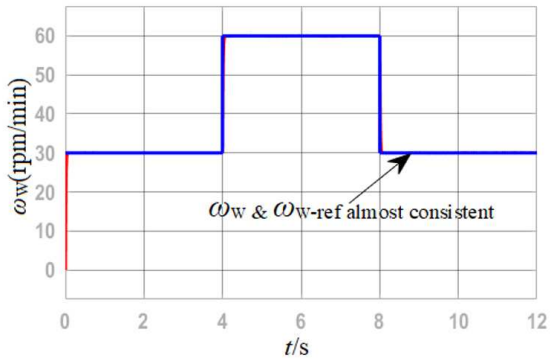

(a) The wind turbine speed waveform based on IMC

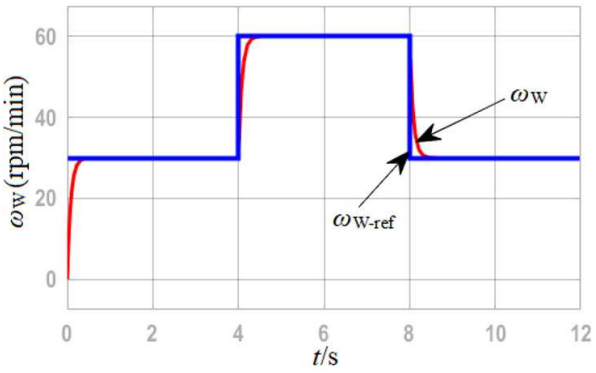

(b) The wind turbine speed waveform based on feedback control

FIGURE 17. The speed waveform of wind turbine based on IMC and equivalent feedback control

As illustrated in Figure 17(a), when $\lambda = 0.01$, the speed waveform of the wind turbine controlled by IMC nearly overlapped with the input speed waveform, and the output tracked the input well. Since the equivalent feedback control based on IMC is only the equivalent transformation of the IMC, both waveforms are consistent when the same λ value is taken with the IMC controller. Additionally, the IMC controller in this example has a single adjustable parameter λ, and the system performance can be adjusted by changing its value. Figure 17(b) shows the wind turbine speed waveform with the increase of λ. The speed tracking performance degrades as the λ increases.

5.4. **Comparison with axial moment observer method in suppressing clearance vibration.** [10] proposes the axial moment observer method, which is another widely used method for suppressing transmission chain clearance vibration by compensating the wind turbine's electromagnetic using the identification value of the axial moment. Figure 18 illustrates the control block diagram for the three-mass transmission chain of the wind power generation system that uses the axial moment observer to suppress vibration. The axial moment observer is shown in the figure's inner portion of the dotted box.

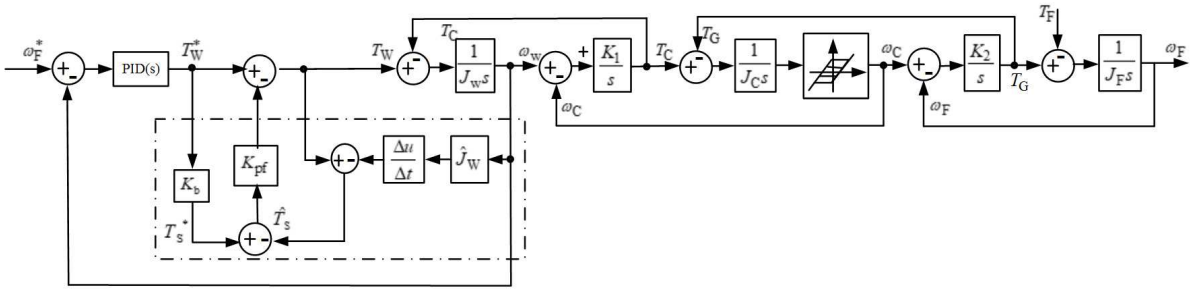

FIGURE 18. The schematic diagram of three-mass wind power generation system controlled by axial moment observer

In Figure 18, $\hat{J}_W$ is the estimated rotational inertia of the wind turbine, T_s is the axial moment of the transmission chain between the wind turbine and the generator, $\hat{T}_s$ is the observed axial moment, T_s^* is the reference torque instruction of the wind turbine T_W^* after the multi-mass block system is equivalent to a single mass block, and K_{pf} is the compensation coefficient, K_b in the figure is

$$K_b = J_F / (J_W + J_F) \tag{24}$$

According to the parameter calculation method in [10], K_b is 1.62, and K_{pf} is 0.6. According to the data in Table 1, $\hat{J}_W$ is 2.6 kg·m^2.

1) Experimental scheme. The simulation experiment system was established according to Figure 18, and the waveform in Figure 19 was obtained by substituting Table 1 and the preceding data.

2) Simulation experiment results and analysis. The waveforms shown in Figures 19(a) and 19(b) are the wind turbine and generator speed waveforms, respectively, for the three-mass transmission chain of the wind power generation system controlled by the

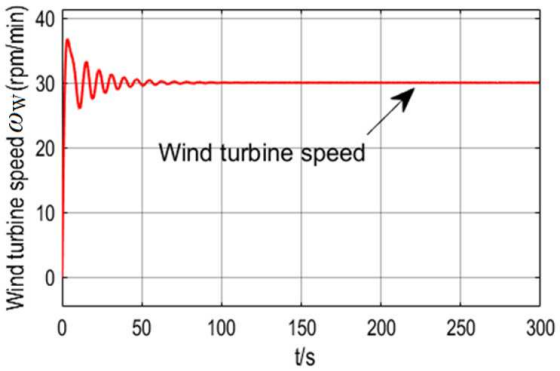

(a) Wind turbine speed waveform

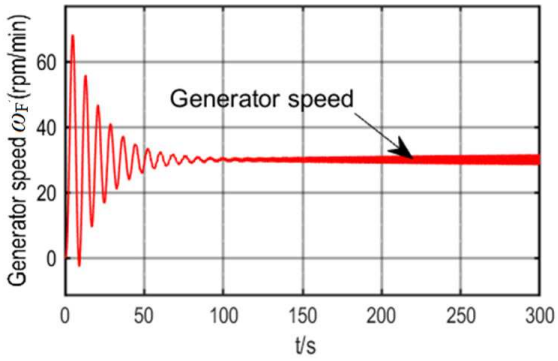

(b) Generator speed waveform

FIGURE 19. The wind turbine and generator speed waveform of the three-mass system by axial moment observer

axial moment observer. As can be seen, both the output speed of the wind turbine and the generator have a significant overshoot, and the generator's output speed vibrates.

Compared with the IMC method illustrated in Figures 16 and 17, the effect of axial moment observer control on generator vibration suppression is not optimal. The IMC method proposed in this paper is extremely effective at suppressing vibrations in a three-mass drive chain.

6. **Conclusion.** The nonlinear vibration of gear clearance is analyzed in this paper using the three-mass transmission chain of a wind power system with clearance as the research object. Since the clearance nonlinear unit N can be decomposed equivalently into a linear unit and a nonlinear bounded disturbance unit, the following work is performed in this paper.

1) A disturbance suppression method based on the IMC principle was proposed to address the nonlinear bounded disturbance presented by the nonlinear unit of gear clearance. The effective disturbance rejection function of IMC suppresses the clearance's nonlinear disturbance factors.

2) We design an IMC and an equivalent feedback speed controller for the wind turbine and generator sides of a three-mass transmission chain in a wind power system and verify their control effect. It is discovered that disturbances of the step, sine wave, and random function have almost no effect on the output. The transmission chain's vibration can be effectively suppressed.

3) It is discovered that applying the IMC method to suppressing transmission chain vibration requires structural diagram transformation, and the controlled object is simplified to a specific IMC structure. It is difficult to transform the IMC structure of a system with more than three masses, and this method is thus limited in its application to multi-mass systems.

4) Intelligent control methods such as intelligent IMC and adaptive neuro-fuzzy reasoning have significant advantages for dealing with the vibration control problem in the presence of model mismatch, and will be applied in further research.

REFERENCES

[1] M. Yang, H. Hu and D. Xu, Cause and suppression of mechanical resonance in PMSM servo system, *Electric Machines and Control*, vol.16, no.1, pp.79-84, 2012.

[2] M. Yang, L. Hao and D. Xu, Online suppression of mechanical resonance based on adapting notch filter, *Journal of Harbin Institute of Technology*, vol.46, no.4, pp.63-69, 2014.

[3] A. Boutros, P. El-Jurdi, H. Y. Kanaan and K. Al-Haddad, Modeling and simulation of a complex mechanical load using the multi-mass approach, *The 17th IEEE Mediterranean Electrotechnical Conference*, Beirut, Lebanon, pp.373-379, 2014.

[4] G. Zhang and J. Hrusho, Vibration control of three-inertia system, *Proc. of the 25th Annual Conference of the IEEE Industrial Electronics Society (IECON'99)*, San Jose, CA, USA, pp.1045-1050, 1999.

[5] S. M. Shahruz, Performance enhancement of a class of nonlinear systems by disturbance observers, *IEEE/ASME Trans. Mechatronics*, vol.5, no.3, pp.319-323, 2000.

[6] F. Miao, H. Shi, X. Zhang et al., Modelling of wind turbines coupled in multi domain and dynamic response analysis, *Proc. of the CSEE*, vol.35, no.7, pp.1704-1712, 2015.

[7] Z. Xu and Z. Pan, Influence of different flexible drive train models on the transient responses of DFIG wind turbine, *2011 International Conference on Electrical Machines and Systems (ICEMS)*, Beijing, China, 2011.

[8] G. Mandic, A. Nasiri, E. Muljadi and F. Oyague, Active torque control for gearbox load reduction in a variable speed wind turbine, *IEEE Trans. Industry Applications*, vol.48, no.6, pp.2424-2432, 2012.

[9] M. Odai and Y. Hori, Speed control of 2-inertial system with gear backlash using gear torque compensator, *1998 IEEE 5th International Workshop on Advanced Motion Control Proceedings (AMC'98)*, Coimbra, Portugal, pp.234-239, 1998.

[10] C. Xia, X. Na, X. Chai and T. Song, Analysis on mechanism and suppression of mechanical resonance in servo system, *Navigation Positioning & Timing*, vol.3, no.1, pp.29-34, 2016.
[11] C. He, X. Zhang, K. Wu and D. Yu, Compensation method for gap of electric servo and engine, *Aerospace Shanghai*, pp.117-121, 2016.
[12] L. Harnefors and H.-P. Nee, Model-based current control of AC machines using the internal model control method, *IEEE Trans. Industry Application*, vol.34, no.1, pp.133-141, 1998.
[13] V. Kongratana, V. Tipsuwanporn, A. Numsomran and A. Detchrat, IMC-based PID controllers design for torsional vibration system, *The 12th International Conference on Control, Automation and Systems*, Jeju, Korea, pp.892-895, 2012.
[14] K. V. Joshi and K. E. Vinodh, Internal model control for regulatory and reference tracking of servo motor, *2019 Innovations in Power and Advanced Computing Technologies (i-PACT)*, DOI: 10.1109/i-PACT44901.2019.8960195, 2019.
[15] Y. Zhou, *Internal Model Control Technology of Induction Motor AC-AC Frequency Conversion Speed Regulation System*, Publishing House of Electronics Industry, Beijing, 2005.
[16] C. Ma, J. Cao and Y. Qiao, Polynomial-method-based design of low-order controllers for two-mass systems, *IEEE Trans. Industrial Electronics*, vol.60, no.3, pp.969-978, 2013.

Author Biography

Chenyang Zhou received the B.S. degree in electrical engineering and its automation from Jiangsu Ocean University, Lianyungang, China, in 2011, and he is currently pursuing the Ph.D. degree in control science and engineering from Jiangnan University, Wuxi, China. He is currently working on Research on Resonance and Suppression of Drive Chain with Transmission Clearance in Wind Power System. His research interests in mechanical resonance suppression on wind power system.

Yanxia Shen received the Ph.D. degree in power electronics and power transmission from China University of Mining and Technology, Xuzhou, China in 2004; she went to the power electronics laboratory of University of California, Irvine for one year's visiting research in September 2007. She is currently a professor and doctoral supervisor at School of Internet of Things Engineering, Jiangnan University. Currently, she is a member of Jiangsu Power Electronics and Power Transmission Professional Committee, director of Jiangsu Electrical Engineering Society, deputy secretary general of Wuxi Automation Society, and a long-term reviewer of "Journal of Electric Machines and Control" and "IEEE Transactions on Power Electronics". She is mainly engaged in the research of power electronics and power transmission technology, new energy technology and teaching of motion control system. She has published more than 60 academic papers in professional journals, among which more than 30 papers are indexed by SCI/EI. She has presided over or participated in 3 National Natural Science Foundation projects and 6 provincial and ministerial key projects. She has won 1 first prize and 1 second prize of provincial and ministerial science and technology progress award. In 2009, she was selected into the Excellent Talents Support Program of the Ministry of Education, and won many honorary titles such as Jiangsu Qingan Project Backstop Teacher and Wuxi Youth Science and Technology Award.

Zaifu Wang received the B.S. degree from Qufu Normal University, Rizhao, China, in 2010, and the Ph.D. degree from Xi'an Jiaotong University, Xi'an, China, in 2019, both in electrical engineering. He has been with Jiangsu Ocean University as a Lecturer since April 2019. His research interests include renewable energy system, high-frequency transformer, hybrid ac/dc microgrid, and high-power converters.